



Application of $\text{LaSr}_2\text{Fe}_2\text{CrO}_{9-\delta}$ in Solid Oxide Fuel Cell Anodes

Jacob M. Haag,^a Brian D. Madsen,^b Scott A. Barnett,^{b,*} and Kenneth R. Poeppelmeier^{a,z}

^aDepartment of Chemistry and ^bDepartment of Materials Science and Engineering, Northwestern University, Evanston, Illinois 60208, USA

The oxide composition $\text{LaSr}_2\text{Fe}_2\text{CrO}_{9-\delta}$ was tested for application as an anode material for solid oxide fuel cells. Despite the high Fe content, this composition was found to be stable under SOFC anode conditions up to $\sim 800^\circ\text{C}$. The composite anode $\text{LaSr}_2\text{Fe}_2\text{CrO}_{9-\delta}-\text{Gd}_{0.1}\text{Ce}_{0.9}\text{O}_{2-\delta}$ was tested in $\text{Gd}_{0.1}\text{Ce}_{0.9}\text{O}_{2-\delta}$ and $\text{La}_{0.9}\text{Sr}_{0.1}\text{Ga}_{0.8}\text{Mg}_{0.2}\text{O}_{3-\delta}$ electrolyte-supported cells in air and humidified H_2 . The maximum power density was $\approx 365 \text{ mW/cm}^2$ at 800°C , with a corresponding total cell resistance of $\approx 0.69 \Omega \text{ cm}^2$. However, the anode polarization resistance at 800°C was $\approx 0.25 \Omega \text{ cm}^2$.
© 2008 The Electrochemical Society. [DOI: 10.1149/1.2836484] All rights reserved.

Manuscript submitted November 12, 2007; revised manuscript received December 19, 2007.
Available electronically January 28, 2008.

Ni–yttria stabilized zirconia (YSZ) cermets are commonly used in solid oxide fuel cell (SOFC) anodes because of their excellent electrochemical performance in hydrogen fuel. However, nickel is susceptible to sulfur poisoning and carbon coking, which are detrimental to anode performance.^{1,2} In order to avoid the challenges associated with Ni metal, several groups have studied conducting oxide materials for application as SOFC anodes. The most successful anodes, in terms of electrochemical performance, have been mixed oxygen-ion and electronically conducting oxides. For example, SOFCs with anodes consisting of the mixed conducting perovskite, $\text{La}_{0.75}\text{Sr}_{0.25}\text{Cr}_{0.5}\text{Mn}_{0.5}\text{O}_{3-\delta}$, yielded a power density of 0.57 W/cm^2 at 800°C with hydrogen fuel.³ Recently, a double perovskite, $\text{Sr}_2\text{MgMoO}_{6-\delta}$, was reported to yield a maximum power density of 0.84 W/cm^2 at 800°C with hydrogen fuel and good sulfur tolerance.^{4,5}

Tao and Irvine have reported that the Cr/Fe-B site perovskite, $\text{La}_{0.75}\text{Sr}_{0.25}\text{Cr}_{0.5}\text{Fe}_{0.5}\text{O}_{3-\delta}$, functions as a stable SOFC anode in H_2 fuel and it is a catalyst for methane reforming and oxidation.⁶ Kozhevnikov et al. characterized, in detail, the mixed conductor, $\text{LaSr}_2\text{Fe}_2\text{CrO}_{9-\delta}$ (LSFeCr), with an oxygen-ion conductivity of 0.03 S/cm at 750°C .⁷ LSFeCr was shown to be stable at oxygen partial pressures as low as $\sim 10^{-21.5} \text{ atm}$ at 750°C ,⁷ which is similar to the operating conditions of intermediate temperature SOFC anodes.

In this paper, the electrochemical performance of composite anodes containing LSFeCr and $\text{Gd}_{0.1}\text{Ce}_{0.9}\text{O}_{2-\delta}$ (GDC) were assessed in GDC and $\text{La}_{0.9}\text{Sr}_{0.1}\text{Ga}_{0.8}\text{Mg}_{0.2}\text{O}_{3-\delta}$ (LSGM) electrolyte-supported SOFCs. GDC was included in the anode because it can decrease the polarization resistance⁸ by introducing triple-phase boundaries and/or providing high-ionic-conductivity pathways within the anode. The anodes were examined after fuel cell testing in order to check their stability in reducing anode conditions.

Experimental

LSFeCr was synthesized by solid-state reaction at 1250°C for 24 h with intermittent grindings. The starting materials were La_2O_3 , SrCO_3 , Fe_2O_3 , and Cr_2O_3 . La_2O_3 was precalcined at 800°C for 4 h to remove all hydroxides. After the synthesis, LSFeCr was attrition milled for 4 h in order to reduce the particle size.

Cell tests were performed on GDC and LSGM electrolyte supported cells. GDC electrolytes were prepared by uniaxially pressing nanoscale GDC (Nextech) and sintering at 1400°C for 6 h, yielding $\sim 300 \mu\text{m}$ thick GDC pellets. For the LSGM electrolytes, La_2O_3 , SrCO_3 , Ga_2O_3 , and MgO were precalcined at 800°C for 4 h to remove all hydroxides and then solid-state reacted at 1250°C for

6 h. The firing was followed by uniaxial pressing and sintering at 1450°C for 6 h, which resulted in $\sim 400 \mu\text{m}$ thick LSGM pellets.

Electrode inks were prepared by ballmilling the powders in ethanol for 24 h, drying, and three-roll milling with a vehicle (Heraeus V737). On the anode side of the LSGM electrolyte, a GDC buffer layer was first screen printed from an ink prepared from nanoscale GDC (Nextech) that had been calcined for 4 h at 800°C ; the buffer layer served to minimize diffusion and/or reactions between LSFeCr and LSGM. The anode active layers were then printed from an ink composed of 50 wt % LSFeCr and 50 wt % GDC. The GDC and LSFeCr–GDC layers were cofired at 1200°C for 1 h. The circular anode active area was 0.5 cm^2 , the GDC layer was $\sim 30 \mu\text{m}$ thick, and the LSFeCr–GDC layer was $\sim 50 \mu\text{m}$ thick. The cathode was composed of 50 wt % $\text{La}_{0.6}\text{Sr}_{0.4}\text{Fe}_{0.8}\text{Co}_{0.2}\text{O}_{3-\delta}$ (LSFeCo, Praxair) and 50 wt % GDC. It was prepared as an ink, screen printed (0.5 cm^2 active area, $\sim 50 \mu\text{m}$ thick), and then fired at 1100°C for 1 h.

For cell testing, gold collector grids were printed over the electrodes and contacted with silver wires. The four-probe single-cell test setup for the current-voltage and electrochemical impedance spectroscopy [(EIS), BAS-Zahner IM-6] measurements has previously been described.⁹ Structural characterization of the electrodes and electrolyte was performed by powder X-ray diffraction on a Scintag diffractometer with $\text{Cu K}\alpha$ radiation and a nickel filter.

Results and Discussion

The anodes were first tested in cells with GDC electrolytes, because no reactions were expected between LSFeCr and GDC. Figure 1a shows a plot of voltage and power density vs current density for different temperatures of a typical cell tested with 97% $\text{H}_2/3\%$ H_2O at the anode and air at the cathode. Open-circuit voltages (OCVs) were relatively low and decreased with increasing temperature, as is typically observed for GDC-electrolyte cells. The cell resistance decreased and maximum power density increased with increasing temperature, with a maximum power density of $\sim 0.3 \text{ W/cm}^2$ at 800°C . The EIS plot in Fig. 1b shows the results obtained at 750°C at a dc cell voltage of 0.45 V. The measurement was done at a voltage lower than open circuit to minimize the electronic current across the mixed-conducting GDC electrolyte.^{10,11} Measurements done at OCV include a relatively large electronic current that effectively short circuits the cell and yields artificially low impedance values for ionic conduction and electrode polarization. It has been shown that EIS data taken from GDC-electrolyte cells at $\leq 0.45 \text{ V}$ provides reasonably accurate values for the electrolyte and electrode impedances.⁸ From the data in Fig. 1b, it is clear that most of the cell resistance is ohmic (given by the left real-axis intercept) and matches reasonably well with the value expected for the $300 \mu\text{m}$ thick GDC electrolyte. The lower-frequency electrode arc did not make a second intercept with the real axis in the frequency range measured.

* Electrochemical Society Active Member.

^z E-mail: krp@northwestern.edu

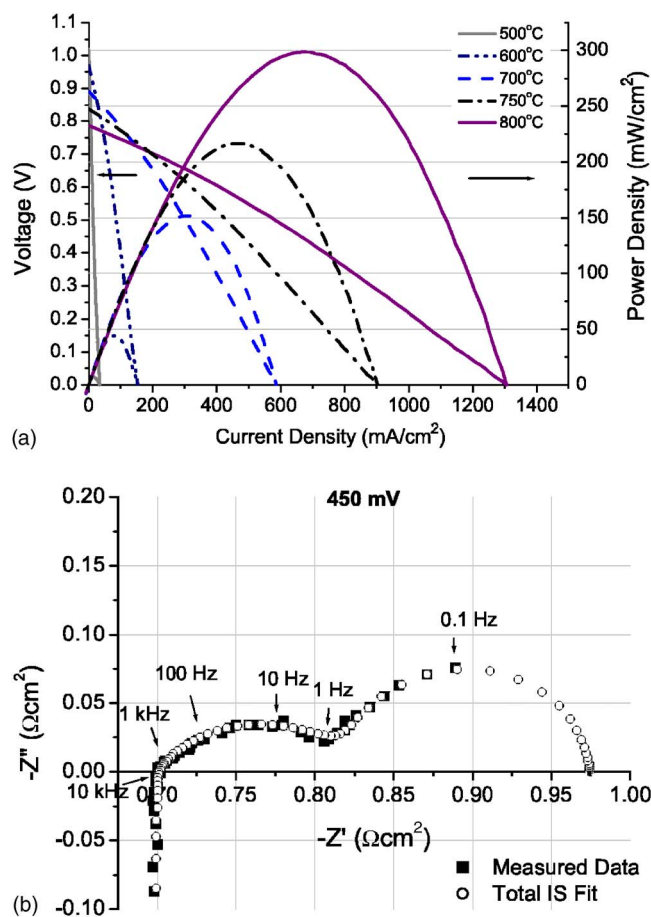


Figure 1. (Color online) (a) Voltage and power density vs current density for a GDC-electrolyte SOFC with a L₂FeCr-GDC composite anode at different temperatures with 97% H₂-3% H₂O fuel and air at the cathode. (b) Electrochemical impedance spectrum for the SOFC measured at 750°C and 0.45 V and an equivalent circuit fit.

The Nyquist plot at 0.45 V was fit with a simple equivalent circuit, $LR_{\text{offset}}(R_2Q_2)(R_{\text{LF}}Q_{\text{LF}})$, where L is an inductance, R is a resistance, Q is a constant phase element, and (RQ) represents a resistor in parallel with a constant phase element. A similar circuit has been used to fit similar cells with lanthanum chromite-based anodes.¹² The medium- and low-frequency arcs, R_2Q_2 and $R_{\text{LF}}Q_{\text{LF}}$, are likely dominated by the L₂FeCr-GDC composite anode. This interpretation is based on the relatively low polarization resistances that have been reported for L₂FeCo-GDC cathodes in YSZ ($\approx 0.01 \Omega \text{ cm}^2$ at 750°C)¹³ and GDC ($\approx 0.07 \Omega \text{ cm}^2$ at 750°C)⁸ electrolyte-supported cells. The fitting was performed using the computer program, *Equivcrt*, by Boukamp and has previously been described in detail.⁹ Based on the fitted arcs, the overall polarization resistance (total width of the arcs) is estimated to be $0.27 \Omega \text{ cm}^2$ at 750°C. The impedance from the L₂FeCo-GDC cathodes has been previously measured to be $\approx 0.07 \Omega \text{ cm}^2$ at 750°C,⁸ so the anode portion of the electrode resistance was $\approx 0.20 \Omega \text{ cm}^2$.

LSGM electrolytes do not exhibit mixed conductivity. Thus, they can provide higher OCVs than GDC-electrolyte cells, and a clearer assessment of anode polarization resistance. Initial SOFC tests were carried out with the L₂FeCr-GDC anode layer printed directly on the LSGM electrolyte. However, it was observed that these cells yielded relatively low power densities, $< 250 \text{ mW/cm}^2$ at 800°C. Thus, we carried out tests where L₂FeCr and LSGM powders were ground together, pressed into a pellet, fired at 1200°C for 6 h, and characterized using X-ray diffraction. The results suggested that cation diffusion may have occurred between the two perovskite phases,

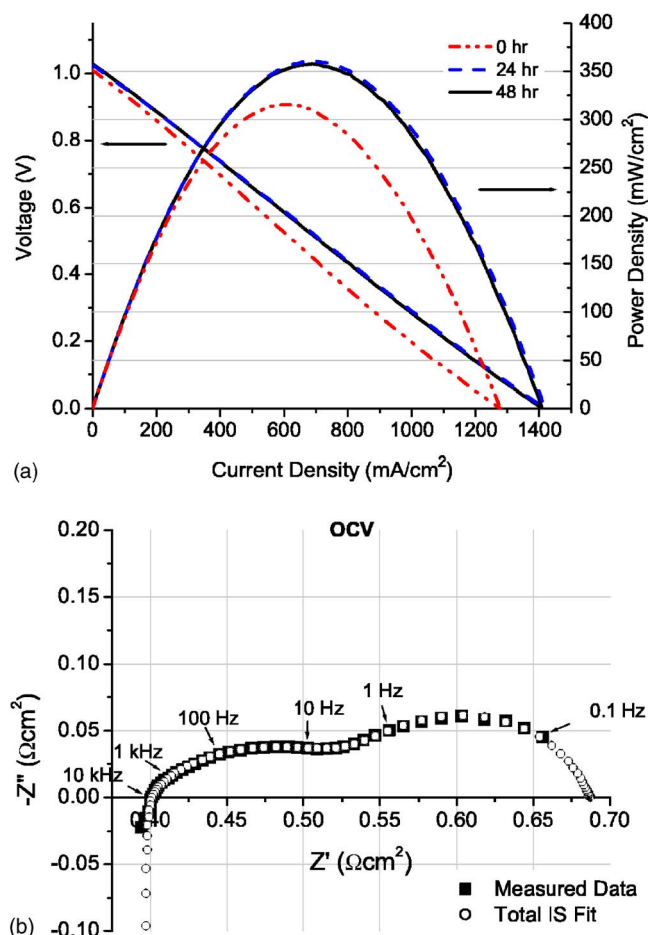


Figure 2. (Color online) (a) A 50 h life test of a LSGM-electrolyte SOFC with a L₂FeCr-GDC composite anode operated at 800°C with 97% H₂-3% H₂O fuel and air at the cathode. (b) Electrochemical impedance spectrum for the SOFC at 800°C measured at open circuit and an equivalent circuit fit.

which could negatively impact cell performance. Therefore, subsequent cells utilized a GDC buffer layer between the anode and the electrolyte to minimize any reactions or interdiffusion.

Figure 2a shows a plot of voltage and power density vs current density at different times during a ~ 50 h test at 800°C with 97% H₂/3% H₂O at the anode and air at the cathode. OCVs were consistently at 1.03 V, much higher than for the GDC-electrolyte cells in Fig. 1. Maximum power density was 0.36 W/cm^2 , higher than the GDC-electrolyte cell primarily due to the higher OCV. The cell performance was also quite stable, after slightly increasing during the initial 24 h of cell testing. The EIS data taken at open circuit from this cell at 800°C, during the period of stable performance, is shown in Fig. 2b. The high-frequency intercept was at $\approx 0.40 \Omega \text{ cm}^2$ and agreed well with the resistance expected for the 0.4 mm thick LSGM electrolyte. The electrode polarization appeared to consist of two separate arcs. Again, the electrode arc was not quite complete in the measured frequency range. The equivalent-circuit fit was again carried out, and the result is shown in Fig. 2b. The fitting of the arcs, R_2Q_2 and $R_{\text{LF}}Q_{\text{LF}}$, gave a total electrode resistance of $0.29 \Omega \text{ cm}^2$. Previous impedance data have shown that L₂FeCo-GDC cathodes have a resistance of $\approx 0.04 \Omega \text{ cm}^2$ at 800°C.⁸ Subtracting the cathode resistance from the total electrode resistance yields an anode polarization resistance of $\approx 0.25 \Omega \text{ cm}^2$ at 800°C. Somewhat surprisingly, this anode resistance is higher than that of the GDC-electrolyte cell anode at 750°C (Fig. 1b). A tentative explanation for this higher resistance is a limited electrode-electrolyte reaction

occurring because of the porous nature of the GDC barrier layer. It is well known that porous ceria barriers, produced by firing at $\sim 1200^\circ\text{C}$ on presintered electrolytes as in the present processing methodology,^{14,15} are not fully effective in preventing such reactions.

The present anodes can be directly compared to $\text{La}_{0.8}\text{Sr}_{0.2}\text{CrO}_3$ -GDC anodes that were tested in cells that were essentially identical to the present cells. These cells gave much lower power densities, $\approx 170 \text{ mW}/\text{cm}^2$ at 800°C , than the LSFerCr-anode SOFCs. The electrode arc at 800°C was clearly much larger, $\approx 0.75 \Omega \text{ cm}^2$, for the chromite anodes.¹² The better performance of the LSFerCr anode can be attributed to the much higher ionic conductivity of this composition compared to $\text{La}_{0.8}\text{Sr}_{0.2}\text{CrO}_3$, which can expand the area of the anode over which electrochemical reactions can occur. The ionic conductivity of LSFerCr is presumably accounted for by the transport of oxygen ions and vacancies between FeO_3 octahedra and $\text{FeO}_{2.5}$ pyramids, as well as the transport of the oxygen ions bridging FeO_3 and CrO_3 octahedra. The conduction of oxygen ions between FeO_3 and CrO_3 octahedra applies at low concentrations of Cr, when the CrO_3 octahedra are isolated from each other. Altering the concentration of Cr in the structure would change the number of CrO_3 octahedra and would likely have an effect on the ionic conductivity.⁷

The present anodes showed area-specific resistances in hydrogen of 0.20 – $0.25 \Omega \text{ cm}^2$ at 750 – 800°C . The SOFC and anode performance was substantially better than in prior reports on a similar composition with lower Fe content, $(\text{La}_{0.75}\text{Sr}_{0.25})(\text{Cr}_{0.5}\text{Fe}_{0.5})\text{O}_{3-\delta}$ tested with YSZ⁶ or LSGM¹⁶ electrolytes and yielding power densities of $\sim 40 \text{ mW}/\text{cm}^2$ at 800 – 900°C and polarization resistances of $\sim 1 \Omega \text{ cm}^2$ at 850 – 900°C (YSZ) and $>1 \Omega \text{ cm}^2$ at 800°C (LSGM). The lower anode polarization can potentially be explained by a higher oxygen-ion conductivity in the present higher-Fe-content material, the use of a composite anode composition rather than the single-phase $(\text{La}_{0.75}\text{Sr}_{0.25})(\text{Cr}_{0.5}\text{Fe}_{0.5})\text{O}_{3-\delta}$, used in the prior reports, or possible reactions between the $(\text{La}_{0.75}\text{Sr}_{0.25})(\text{Cr}_{0.5}\text{Fe}_{0.5})\text{O}_{3-\delta}$ and LSGM or YSZ that were minimized in the present work by using a GDC electrolyte or barrier layer. The present anode performance was similar to the best reported ceramic anodes: 0.1 – $0.25 \Omega \text{ cm}^2$ for $\text{Sr}_2\text{Mg}_{1-x}\text{Mn}_x\text{MoO}_{6-\delta}$ ($x = 0$ – 1) at 800°C ,⁴ $0.25 \Omega \text{ cm}^2$ for $\text{La}_{0.75}\text{Sr}_{0.25}\text{Cr}_{0.5}\text{Mn}_{0.5}\text{O}_3$ anodes at 925°C (with a $\text{Ce}_{0.8}\text{Gd}_{0.2}\text{O}_{2-\delta}$ interlayer),^{6,17} $0.2 \Omega \text{ cm}^2$ for cerium-modified $(\text{La},\text{Sr})(\text{Ti},\text{Ce})\text{O}_3$ anodes at 850°C ,¹⁸ and $0.20 \Omega \text{ cm}^2$ for $\text{La}_{0.8}\text{Sr}_{0.2}\text{Cr}_{0.82}\text{Ru}_{0.18}\text{O}_3$ anodes at 800°C .^{12,19}

The LSFerCr-GDC anodes were examined by X-ray diffraction after cell testing to test for possible decomposition under highly reducing anode conditions. Figure 3 shows the diffraction pattern from the anode after the 50 h cell test at 800°C . LSFerCr and LSGM were both identified; however, because they are both perovskites with similar size cations, the peaks were highly overlapped. A trace amount of $\text{SrLaGa}_3\text{O}_7$ was present, which is a commonly formed second phase in LSGM electrolytes. GDC from the anode and buffer layer and Au from the current collector grid were also identified. No intensity was observed at the positions expected for elemental Fe, the expected major product of LSFerCr decomposition. Thus, the LSFerCr perovskite structure remained intact under SOFC operating conditions. Prior results indicated that LSFerCr begins to decompose at $p\text{O}_2$ values $< 10^{-20}$ atm at 800°C , quite close to the conditions in the SOFC test. The calculated $p\text{O}_2$ value for humidified hydrogen (97% $\text{H}_2/3\% \text{H}_2\text{O}$) at 800°C is $\sim 10^{-22}$ atm, suggesting that LSFerCr decomposition might be expected. However, the cell current during the SOFC life test presumably increased the H_2O content, increasing $p\text{O}_2$ within the anode.

Conclusions

Initial cell tests demonstrate that the composite, LSFerCr-GDC, is a promising SOFC anode. Power densities of 300 – $360 \text{ mW}/\text{cm}^2$ and anode polarization resistances of 0.20 – $0.25 \Omega \text{ cm}^2$ were measured at 750 – 800°C . Additional work can be done to determine the

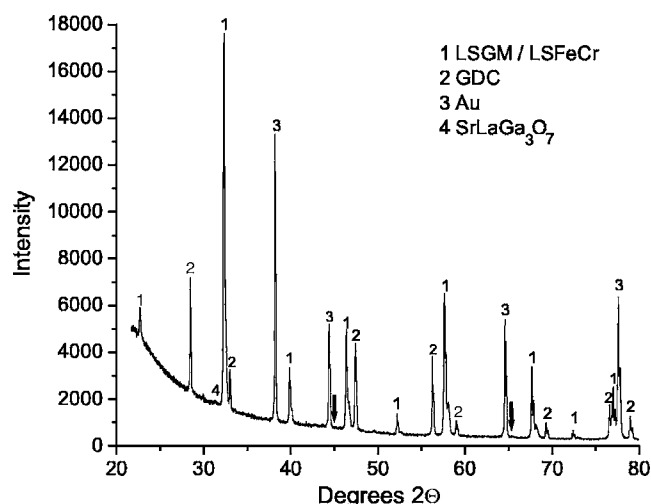


Figure 3. XRD pattern of a LSFerCr-GDC anode after testing the SOFC at 800°C for 50 h. The arrows indicate where iron metal (PDF no. 06-0696) intensity would be expected.

fuel flexibility of the anode and the optimal composition by varying the LSFerCr:GDC ratio. Also, longer-term cell tests are needed to determine the long-term stability and performance of the anode.

Acknowledgments

The authors gratefully acknowledge the financial support of the Department of Energy (contract no. DE-FG02-99ER14999) and the use of the Central Facilities supported by the MRSEC program of the National Science Foundation (grant no. DMR-0576097) at the Materials Research Center of Northwestern University.

Northwestern University assisted in meeting the publication costs of this article.

References

1. Y. Matsuzaki and I. Yasuda, *Solid State Ionics*, **132**, 261 (2000).
2. C. M. Finnerty, N. J. Coe, R. H. Cunningham, and R. M. Ormerod, *Catal. Today*, **46**, 137 (1998).
3. J. Pena-Martinez, D. Marrero-Lopez, J. C. Ruiz-Morales, C. Savaniu, P. Nunez, and J. T. S. Irvine, *Chem. Mater.*, **18**, 1001 (2006).
4. Y. H. Huang, R. I. Dass, Z. L. Xing, and J. B. Goodenough, *Science*, **312**, 254 (2006).
5. Y. H. Huang, R. I. Dass, J. C. Denyszyn, and J. B. Goodenough, *J. Electrochem. Soc.*, **153**, A1266 (2006).
6. S. W. Tao and J. T. S. Irvine, *Chem. Mater.*, **16**, 4116 (2004).
7. V. L. Kozhevnikov, I. A. Leonidov, J. A. Bahteeva, M. V. Patrakeev, E. B. Mitberg, and K. R. Poeppelmeier, *Chem. Mater.*, **16**, 5014 (2004).
8. B. D. Madsen and S. A. Barnett, *J. Electrochem. Soc.*, **154**, B501 (2007).
9. B. D. Madsen and S. A. Barnett, *Solid State Ionics*, **176**, 2545 (2005).
10. M. Mogensen, N. M. Sammes, and G. A. Tompsett, *Solid State Ionics*, **129**, 63 (2000).
11. M. L. Liu and H. X. Hu, *J. Electrochem. Soc.*, **143**, L109 (1996).
12. B. D. Madsen, W. Kobsiriphat, Y. Wang, L. D. Marks, and S. A. Barnett, in *SOFC Anode Performance Enhancement Through Precipitation of Nanoscale Catalysts*, K. Eguchi, S. C. Singhal, H. Yoko Kawa, and J. Mizusaki, Editors, SOFC X, Nara, Japan, The Electrochemical Society, Pennington, NJ, p. 1339 (2007).
13. E. P. Murray, M. J. Sever, and S. A. Barnett, *Solid State Ionics*, **148**, 27 (2002).
14. S. P. Simmer, J. F. Bonnett, N. L. Canfield, K. D. Meinhardt, V. L. Sprenkle, and J. W. Stevenson, *Electrochem. Solid-State Lett.*, **5**, A173 (2002).
15. M. Becker, A. Mai, E. Ivers-Tiffée, and F. Tietz, in *Long-Term Measurements of Anode-Supported Solid Oxide Fuel Cells with LSCF Cathodes under Various Operating Conditions*, S. C. Singhal and J. Mizusaki, Editors, SOFC IX, Quebec, The Electrochemical Society, Pennington, NJ, p. 514 (2005).
16. J. Pena-Martinez, D. Marrero-Lopez, D. Perez-Coll, J. C. Ruiz-Morales, and P. Nunez, *Electrochim. Acta*, **52**, 2950 (2007).
17. S. W. Tao and J. T. S. Irvine, *J. Electrochem. Soc.*, **151**, A252 (2004).
18. O. A. Marina and L. R. Pederson, in *Novel Ceramic Anodes for SOFCs Tolerant to Oxygen, Carbon and Sulfur*, p. 481, The Fifth European Solid Oxide Fuel Cell Forum, Lucerne, J. Huijsmans, Editor, European Fuel Cell Forum, Oberrohrdorf, Switzerland (2002).
19. B. D. Madsen, W. Kobsiriphat, Y. Wang, L. D. Marks, and S. A. Barnett, *J. Power Sources*, **166**, 64 (2007).